Properties of the nonlinear Schrödinger equation on a lattice

Rainer Scharf and A. R. Bishop
Theoretical Division and Center for Nonlinear Studies, Los Alamos National Laboratory, Los Alamos, New Mexico 87545
(Received 8 November 1990)

We add an on-site potential to the integrable lattice nonlinear Schrödinger equation and show how a number of interesting and novel features can be understood with the help of a simple soliton collective variable approximation. Results include: trapping of a soliton in a linear potential and on a *maximum* of a smooth potential; trapping of a soliton on a repulsive impurity and breaking into two solitons beyond a critical impurity strength; and a crossover from a soliton state to a local impurity mode upon increasing the strength of an attractive potential. In addition, we prove and illustrate the complete integrability of the system for a linear on-site potential. Results are compared with those for a nonintegrable discretization of the cubic Schrödinger equation.

I. INTRODUCTION

Understanding the interplay between *disorder* and *nonlinearity* is of fundamental importance in many physical contexts, and this combination of ingredients raises a number of unsolved mathematical questions.[1] The last three decades have seen enormous progress in identifying the essential roles of nonlinearity and disorder separately. Each may lead to self-localized excitations—"soliton"-like structures due to nonlinearity and "Anderson localization" due to disorder. It is therefore natural to ask how these effects might reinforce, complement, or frustrate each other. In particular, we need to understand their combined roles in transport and transmission coefficients. Do solitons behave as "particles" in the presence of disorder, for instance, or interact very strongly with other degrees of freedom? Does the randomness of deterministic chaos mimic that produced by stochastic external forces? These and other issues are of great experimental concern in fields from nonlinear optics,[2] to polaron formation in solid-state materials,[3,4] to vibron localization in natural and synthetic biomolecules.[5–7]

Disorder may be parametric or additive, temporal or spatial. Furthermore, the "color" of the noise or disorder is often relevant. As a first step, in this program, we consider the discrete nonlinear Schrödinger equation in $(1+1)$ dimensions and investigate some elementary forms of parametric spatial disorder—namely, constant bias, isolated impurities, and periodic spatial variations. Several novel features have been found as a result of the *discreteness* of the lattice, and it is these on which we wish to focus here.

Over the years, it has been demonstrated that a certain set of completely integrable, soliton-bearing, partial differential equations can be very useful models for the effects of nonlinearity in the absence of disorder. Despite their exact integrability, they contain enough of the essential physical ingredients to represent the dominant behavior of many nearby equations. The nonlinear Schrödinger equation is perhaps the most ubiquitous of these exact soliton systems,[5] modeling self-localization, self-trapping, and self-focusing phenomena. On the other hand, tight-binding models have proved to be important for gaining insight into the effect of disorder in "linear" solid-state problems (Anderson model, Hubbard model): It is therefore natural to modify these models to incorporate nonlinearity effects. Among such models is the so-called self-trapping of electrons in ionic crystals through polaronic lattice distortion.[3] (The same equation models self-trapping in many other coupled-field situations.[6,7]) A simple adiabatic way to model this self-interaction via lattice distortion in the tight-binding approximation is through the *lattice* nonlinear Schrödinger equation

$$i\dot{\psi}_n = -\psi_{n+1} - \psi_{n-1} + 2\kappa|\psi_n|^2\psi_n + V_n\psi_n \ , \tag{1}$$

where $|\psi_n(t)|^2$ is proportional to the electron density at site n and time t; $\kappa = \pm 1$, leading to repulsive (attractive) self-interaction; the dot stands for the derivative with respect to time t; V_n is an on-site potential that the electrons experience, e.g., arising from impurities in the lattice. In the continuum limit Eq. (1) with $V_n = 2$ leads to the completely integrable nonlinear Schrödinger (NLS) equation with soliton or "dark-soliton" solutions for $\kappa = -1$ and $+1$, respectively.[2]

It is well known that Eq. (1) (for $V_n = 2$) is a *nonintegrable* discretization of the completely integrable continuum NLS equation. Instead, in Sec. II we introduce a different discretization which is *integrable* and allows us to compare the effect of on-site potentials with the known analytic behavior of the unperturbed dynamics. In the case of the integrable discretization, $|\psi_n|^2$ can no longer be interpreted as a local density. We do not introduce this integrable version because of its superior physical relevance, but rather in the spirit of soliton equations noted earlier. However, it is worth noting that the integrable model is widely studied for its interesting (classical and quantum) features in its own right.

In some respects the integrable and nonintegrable discetizations, of course, lead to different behavior.[8] On the other hand, we find that certain distinctive features of the *discreteness* in the integrable model are preserved in the nonintegrable case. These features seem to have general relevance, but their investigation is greatly facilitated by

the integrability of the model in question.

In this article we show how the *interplay* of discreteness, nonlinearity, and a site-dependent on-site potential gives rise to some novel effects, even in the absence of global disorder. Our main intention is to illustrate four important points: (i) There are some interesting qualitative features of the solutions of the discrete integrable NLS in the presence of disorder (e.g., isolated impurities, spatially periodic or random on-site potentials); (ii) there are novel effects of discretization, particularly the existence of upper and lower potential bounds for the motion of NLS solitons; (iii) a simple soliton collective coordinate approximation gives an extremely robust ansatz for the treatment of the dynamics in the presence of the above-mentioned perturbations; and (iv) the stationary solution approach, familiar in the disordered linear Schrödinger equation, is incomplete in the discussion of the disordered NLS, where the full space-time dynamics must be treated.

After introducing the nonintegrable and integrable discretizations and their Poissonian structures in Sec. II, we discuss exact traveling solutions of the integrable system in Sec. III. In Sec. IV we address the influence of slowly varying on-site potentials and treat this case by a collective variable approximation. We find that solitons can be trapped in a linear potential and on a *maximum* of a smooth potential. This property of the discretization holds in both the integrable and nonintegrable cases. In Sec. V we construct traveling solutions for the integrable discretization with on-site potentials depending linearly on the spatial coordinate. Then we show that the collective variable approximation is exact in this case. Numerical evidence for the complete integrability of the system with a linear potential is given in the form of previously unobserved time-periodic two-soliton collisions. Finally, the complete integrability is proven analytically. Section VI discusses the interaction of a soliton with attractive and repulsive single-site impurities: a crossover from a soliton (i.e., nonlinearity-dominated) state to a local impurity (i.e., disorder-dominated) mode upon increasing the strength of an attractive potential, and the (dynamic) trapping of a soliton on a repulsive impurity and breaking into two solitons beyond a critical impurity strength. Finally, Sec. VII gives a summary and outlook.

II. TWO DIFFERENT DISCRETIZATIONS

The discrete model given by Eq. (1) can be derived from the Hamiltonian

$$H_1=-\sum_{n=-\infty}^{\infty}(\psi_n\psi_{n+1}^*+\psi_n^*\psi_{n+1}) +\kappa\sum_{n=-\infty}^{\infty}|\psi_n|^4+\sum_{n=-\infty}^{\infty}V_n|\psi_n|^2 , \tag{2}$$

with the Poisson brackets

$$\{\psi_m,\psi_n^*\}=i\delta_{mn},\quad \{\psi_m,\psi_n\}=\{\psi_m^*,\psi_n^*\}=0 , \tag{3}$$

and the equation of motion

$$\dot{\psi}_n=\{H_1,\psi_n\} . \tag{4}$$

From Eq. (2) it is apparent that κ positive (negative) amounts to repulsive (attractive) self-interaction. The Hamiltonian H_1 and Eq. (1) are both invariant under global phase change. The corresponding generator, the norm N_1, is therefore conserved:

$$\dot{N}_1=0 \text{ with } N_1=\sum_n|\psi_n|^2 . \tag{5}$$

Equation (1) is not completely integrable, even for $V_n=$const (as opposed to its continuum limit), leading to complex behavior in space and time. Indeed, recent investigations of the spatial properties of time periodic solutions $\psi_n(t)=e^{-i\omega t}\chi_n$ of Eq. (1) for $\kappa=-\lambda/2<0$ show that the (complex) amplitudes χ_n are connected by a nonintegrable symplectic map.[9] Therefore, the powerful theorems of nonlinear dynamics, like the Kolmogorov-Arnold-Moser (KAM) theorem,[10] apply, although it is important to explore the *full* time dependence, as we do below.

As Eq. (1) is nonintegrable for arbitrary potential V_n, it is not so easy to compare the effects of a nonconstant V_n with a constant one analytically in cases where the integrable continuum limit approximation does not hold. However, there exists a second lattice NLS equation, which is completely integrable for constant V_n:[11,12]

$$i\dot{\psi}_n=-(\psi_{n+1}+\psi_{n-1})(1-\kappa|\psi_n|^2)+V_n\psi_n . \tag{6}$$

Comparison with Eq. (1) shows that $2\psi_n$ has been replaced by $\psi_{n+1}+\psi_{n-1}$ in the cubic term. Equation (6) can be derived from the Hamiltonian

$$H=-\sum_n(\psi_n\psi_{n+1}^*+\psi_n^*\psi_{n+1}) -\frac{1}{\kappa}\sum_n V_n\ln(1-\kappa|\psi_n|^2) , \tag{7}$$

with the nonstandard Poisson brackets

$$\{\psi_m,\psi_n^*\}=i(1-\kappa|\psi_n|^2)\delta_{mn} ,\quad \{\psi_m,\psi_n\}=\{\psi_m^*,\psi_n^*\}=0 , \tag{8}$$

and $\kappa=\pm1$. For $\kappa=1$, we assume $|\psi_n|<1$.

If V_n is constant, Eq. (6) is completely integrable and possesses an infinity of independent conserved quantities which are in involution with the Hamiltonian H. For nonconstant on-site potential V_n, Eq. (6) is no longer completely integrable in general (see below). However, at least one integral of motion (besides H) still exists:

$$N=-\frac{1}{\kappa}\sum_n\ln(1-\kappa|\psi_n|^2) , \tag{9}$$

playing the role of a norm.

From now on we set $\kappa=-1$ (attractive self-interaction) and observe that, by rescaling $\psi_n(t)$ with $\sqrt{\lambda}$ for $\lambda>0$, Eq. (6) takes the form

$$i\dot{\psi}_n=-(\psi_{n+1}+\psi_{n-1})(1+\lambda|\psi_n|^2)+V_n\psi_n . \tag{10}$$

Therefore, it will be sufficient to investigate Eq. (10) for $\lambda=1$.

III. EXACT SOLUTIONS AND THEIR INTEGRALS

For a vanishing potential ($V_n \equiv 0$), traveling and oscillating solutions are easily found to be either of the form

$$\psi_n(t) = A\ \mathrm{cn}(\beta(n-ut-x_0),k)e^{-i(\omega t+\alpha n+\phi_0)}\ , \quad (11)$$

with amplitude A, frequency ω, and velocity u given by

$$\begin{aligned} A &= \frac{k\ \mathrm{sn}(\beta,k)}{\mathrm{dn}(\beta,k)}\ , \\ \omega &= -\frac{2\ \mathrm{cn}(\beta,k)\cos\alpha}{\mathrm{dn}^2(\beta,k)}\ , \\ u &= -\frac{2\ \mathrm{sn}(\beta,k)\sin\alpha}{\beta\ \mathrm{dn}(\beta,k)}\ , \end{aligned} \quad (12)$$

or of the form gained upon interchanging cn and dn in Eqs. (11) and (12) and rescaling A by k^{-1}. The parameters α, β, and k have the following ranges: $-\pi \le \alpha \le \pi$, $0 < \beta < \infty$, and $0 < k < 1$. For $k \to 0$ and $\beta = 0$, the phonon dispersion relation is recovered: $\omega = -2\cos\alpha$. For $0 < k < 1$ the solutions (11) are phononlike, whereas for $k \to 1$ they are one-soliton solutions:

$$\begin{aligned} \psi_n(t) &= \sinh\beta\ \mathrm{sech}[\beta(n-ut-x_0)]e^{-i(\omega t+\alpha n+\phi_0)}\ , \\ \omega &= -2\cosh\beta\cos\alpha\ , \\ u &= -\frac{2\sinh\beta\sin\alpha}{\beta}\ . \end{aligned} \quad (13)$$

The form (13) implies that narrow solitons travel faster than wider ones having the same α.

As the energy $E = H$ and the norm N for the one-soliton solutions (13) are invariant under *continuous* translations, they are easily found by integration:

$$\begin{aligned} E &= -\sum_n (\psi_n \psi_{n+1}^* + \psi_n^* \psi_{n+1}) = -4\sinh\beta\cos\alpha\ , \\ N &= \sum_n \ln[1+\sinh^2\beta\ \mathrm{sech}^2(\beta n)] \\ &= \int_{-\infty}^{+\infty} \ln[1+\sinh^2\beta\ \mathrm{sech}^2(\beta x)]dx \\ &= 2\beta\ . \end{aligned} \quad (14)$$

The last line implies that narrow solitons have larger norms than wider ones.

Upon imposing periodic boundary conditions ($\psi_{n+L} \equiv \psi_n$ with $L = l_{\mathrm{chain}}$), the strict soliton solutions are excluded and only k values are allowed for which $\beta L = 4mK(k)$, where m gives the number of humps the solution has. However, by increasing β the modulus k can be arbitrarily close to 1, and the corresponding solutions for $m = 1$ are practically indistinguishable from isolated solitons.

IV. SLOWLY VARYING ON-SITE POTENTIALS

If we place the one-soliton solution (13) for $t = 0$ as an initial excitation into Eq. (10) with a nonconstant potential V_n, we do not expect Eq. (13) to describe the evolution for $t > 0$. But under certain conditions, namely, if the potential varies slowly over the soliton hump, we expect a one-soliton solution (13) with time-dependent parameters $\alpha(t)$ and $\beta(t)$ to be a good approximation to the exact, unknown solution of Eq. (10). This so-called "collective variable approximation" or "adiabatic approximation," well known in the continuum limit, seems to work extremely well in the lattice case, as shown by the numerical evidence which we present below.

For $V_n = V = \mathrm{const}$, we observe

$$\begin{aligned} E &= -4\sinh\beta\cos\alpha + VN\ , \\ N &= 2\beta\ . \end{aligned} \quad (15)$$

Now we assume V_n varying so slowly with n that, within a good approximation, the soliton of width β^{-1} feels only a constant potential: $V_{n+1} - V_n \ll \beta V_n$. Whether the radiative decay of the soliton is weak enough that the use of collective variables makes sense may be decided either perturbatively[13] or by inspecting numerical simulations.

Introducing the notation $V(x)$ for the slowly varying potential V_n ($n = x$), we see from Eq. (15) that under the assumptions made above the soliton does not change shape ($N = 2\beta$ is independent of V) and changes of the local potential $V(x)$ lead to changes of α only:

$$E = -4\sinh\beta\cos\alpha(x) + 2\beta V(x) = \mathrm{const}\ . \quad (16)$$

The spatial *discreteness* of the model under investigation now leads to an interesting effect. As $|\cos\alpha(x)| \le 1$, there exist *upper* and *lower* bounds for the potential that the soliton can enter, depending on the initial condition $E = -4\sinh\beta\cos\alpha_0 + 2\beta V_0$:

$$E = -4\sinh\beta + 2\beta V_{\max} = 4\sinh\beta + 2\beta V_{\min}\ , \quad (17)$$

leading to

$$\begin{aligned} V_{\max} - V_0 &= \frac{2\sinh\beta}{\beta}(1-\cos\alpha_0)\ , \\ V_0 - V_{\min} &= \frac{2\sinh\beta}{\beta}(1+\cos\alpha_0)\ . \end{aligned} \quad (18)$$

In the continuum limit, the unusual lower bound disappears.

To integrate the differential-difference equations (1) and (10) numerically, we used a fifth- and sixth-order Runge-Kutta-Verner method and checked the accuracy using the conserved quantities H and N given by Eqs. (2), (5), (7), and (9). These were conserved to a relative error less than 10^{-4}.

Figure 1 shows two cases where the soliton is trapped in a linearly increasing potential V_n between $V_{\min}$ and $V_{\max}$. Figure 2 shows the same cases, but for the nonintegrable discreteness [Eq. (1)] for comparison. Although in the latter case the soliton decays quite rapidly, it refocuses. The total structure remains localized and spreads only very slowly. $V_{\min\,(\max)}$ in Eq. (18) give a good estimate for the size of the structure after the first reemergence. Figure 3 shows that the soliton can be trapped in a minimum of $V(x)$ as well as on a maximum [$V_n = \mp 2\cos(\pi n/52)$ in Eq. (6)]. Again, in both cases the turning points of the soliton motion are well approximated by $V_{\min\,(\max)}$.

The soliton might be regarded as a particle moving in an effective potential $V_{\mathrm{eff}}(x)$, which can be found as fol-

lows [$u(x)=-2\sinh\beta\sin\alpha(x)/\beta$ is the soliton velocity at position x]:

$$\frac{u^2}{2}+\frac{V(x)[\beta V(x)-E]}{2\beta}=\frac{16\sinh^2\beta-E^2}{8\beta^2}\ , \tag{19}$$

where $V_{\rm eff}(x)=(1/2\beta)V(x)[\beta V(x)-E]$ plays the role of the effective potential and the right-hand side of Eq. (19) plays the role of the particle energy, both depending on the initial conditions. This explains the apparent paradox of a soliton trapped on a maximum of $V(x)$: The effective potential experienced by the soliton is not simply this externally applied one.

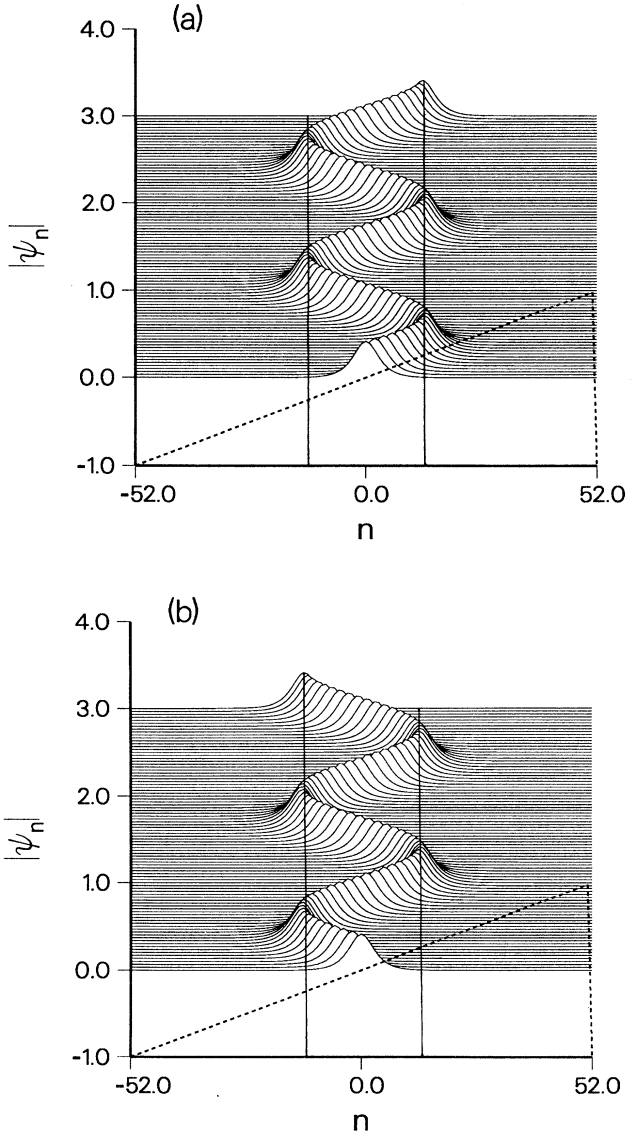

FIG. 1. Soliton trapping on a tilted plane: Solution of Eq. (6), for $l_{\rm chain}=104$; zero boundary conditions; $V_n=16n/l_{\rm chain}$; initial soliton parameters: $\beta=0.4$, (a) $\alpha=-1.571$ and (b) $\alpha=1.571$; integration time $T=90$. The vertical marks indicate the turning points given by Eq. (18), the dashed lines indicate the form of the potential.

V. LINEAR ON-SITE POTENTIALS

Specializing to $V(x)=an+b$ for $a\neq 0$, one can easily verify that the solutions corresponding to Eq. (11) are of the following form:

$$\psi_n(t)=A\ \mathrm{cn}(\beta[n-x(t)],k)e^{-i[\phi(t)+\alpha(t)n+bt]}\ , \tag{20}$$

with A given by Eq. (12), and

$$\begin{aligned}\alpha(t)&=at+\alpha_0\ ,\\ \phi(t)&=-\frac{2\,\mathrm{cn}(\beta,k)}{a\,\mathrm{dn}^2(\beta,k)}[\sin\alpha(t)-\sin\alpha_0]+\phi_0+bt\ ,\\ x(t)&=\frac{2\,\mathrm{sn}(\beta,k)}{a\beta\,\mathrm{dn}(\beta,k)}[\cos\alpha(t)-\cos\alpha_0]+x_0\ .\end{aligned} \tag{21}$$

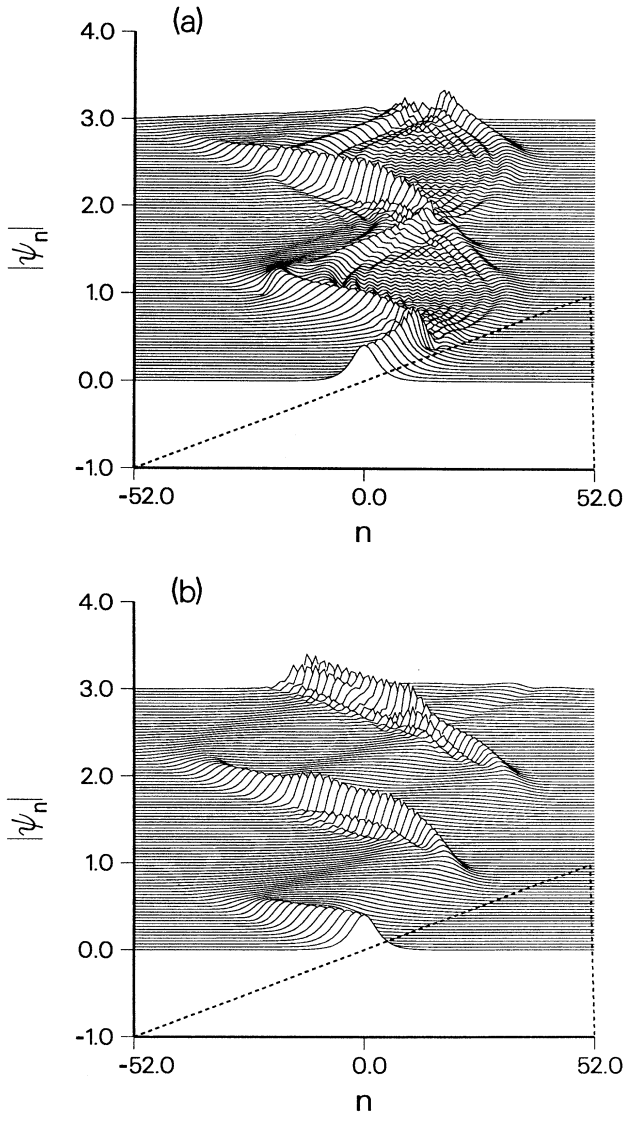

FIG. 2. Trapping for nonintegrable dynamics: Solution of Eq. (1), for $l_{\rm chain}=104$; zero boundary conditions; $V_n=16n/l_{\rm chain}$; initial soliton parameters: $\beta=0.4$, (a) $\alpha=-1.571$ and (b) $\alpha=1.571$; integration time $T=90$.

For $k \to 1$ this leads to oscillating soliton solutions (to simplify expressions we have taken $\alpha_0 = \phi_0 = 0$)

$$\psi_n(t) = \sinh\beta \,\mathrm{sech}\{\beta[n - x(t)]\} e^{-i[\phi(t) + V_n t]} ,$$
$$\phi(t) = -\frac{2}{a}\cosh\beta \sin(at) + bt , \tag{22}$$
$$x(t) = \frac{2}{a\beta}\sinh\beta[\cos(at) - 1] + x_0 .$$

This shows that for a linear potential $V_n = an + b$ the values for $V_{\max}$ and $V_{\min}$ given by Eq. (18), as well as the collective variable description of the soliton motion by Eq. (19), are exact.

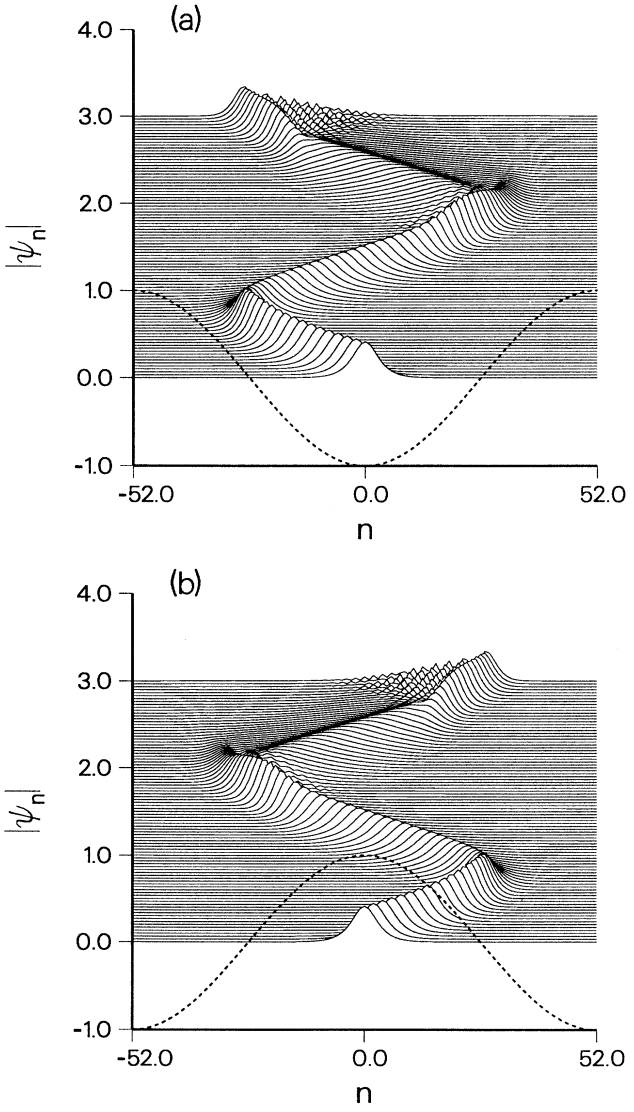

FIG. 3. Soliton trapping on potential minima and maxima: Solution of Eq. (6), for $l_{\text{chain}} = 104$; periodic boundary conditions; $V_n = \mp 2\cos(2\pi n / l_{\text{chain}})$ [(a) and (b), respectively]; initial soliton parameters: $\beta = 0.4$, (a) $\alpha = 1.571$ and (b) $\alpha = -1.571$; integration time $T = 90$.

As Eq. (6) is completely integrable for constant V_n, asymptotically for $t \to \pm\infty$ solitons suffer only phase shifts if their paths cross (see Fig. 4). Remarkably, even for a linear on-site potential V_n, solitons emerge intact from a two-soliton collision. This is shown most strikingly in Fig. 5, which should be compared with Fig. 1. These two-soliton collisions show a notable feature: They are periodic in time. This is clearly a discreteness effect and should be contrasted with the behavior in the continuum limit.[14]

Although the motion of the solitons in Fig. 5 is completely different from the straight-line behavior for the completely integrable system with constant potential, the solitons interact in a way which is typical for a completely integrable system. This raises the interesting question of whether Eq. (10) is completely integrable for $V_n = an + b$, which we now discuss.

It is known that the spatially continuous NLS equation is completely integrable even for on-site potentials linear or quadratic in the spatial variable.[14,15] We now prove that Eq. (6) for a linear potential $V_n = an + b$ is also completely integrable by casting it in the form of a zero-curvature condition with time-dependent spectral parameter λ. Following Ref. 12, the compatibility condition for a vector $F_n(t, \lambda(t))$, obeying the equations

$$F_{n+1} = L_n(t,\lambda) F_n ,$$
$$\frac{dF_n}{dt} = W_n(t,\lambda) F_n , \tag{23}$$

is of the following form:

$$\frac{d}{dt} L_n + L_n W_n - W_{n+1} L_n = 0 . \tag{24}$$

With the choice

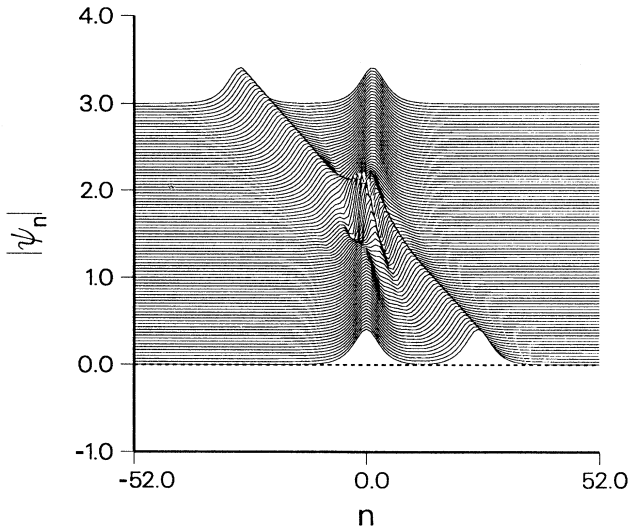

FIG. 4. Two-soliton collision: Solution of Eq. (6), for $l_{\text{chain}} = 104$; periodic boundary conditions; $V_n = 0$; initial soliton parameters: $\alpha_1 = 0$, $\alpha_2 = 1.0$, and $\beta_1 = \beta_2 = 0.4$; integration time $T = 90$.

$$L_n(t,\lambda)=\begin{bmatrix}\lambda & \sqrt{\kappa}\psi_n^* \\ \sqrt{\kappa}\psi_n & \lambda^{-1}\end{bmatrix},$$
$$W_n(t,\lambda)=i\begin{bmatrix}1+\kappa\psi_n^*\psi_{n-1}-\lambda^2+f_n & \sqrt{\kappa}(\lambda^{-1}\psi_{n-1}^*-\lambda\psi_n^*) \\ \sqrt{\kappa}(\lambda^{-1}\psi_n-\lambda\psi_{n-1}) & -1-\kappa\psi_n\psi_{n-1}^*+\lambda^{-2}-f_n\end{bmatrix}, \tag{25}$$

the zero-curvature condition (24) leads to

$$f_n=\gamma n+\delta\ ,$$
$$\lambda(t)=\lambda_0 e^{i\gamma t}\ , \tag{26}$$
$$V_n=2+f_n+f_{n+1}=2\gamma n+2(\delta+1)+\gamma=an+b\ ,$$

$$i\dot{\psi}_n=-(\psi_{n+1}+\psi_{n-1})(1-\kappa|\psi_n|^2)+V_n\psi_n\ .$$

This proves the complete integrability of Eq. (6) for linear potentials. Whether Eq. (6) is also integrable for quadratic potentials, as in the continuum case,[14] deserves further investigation.

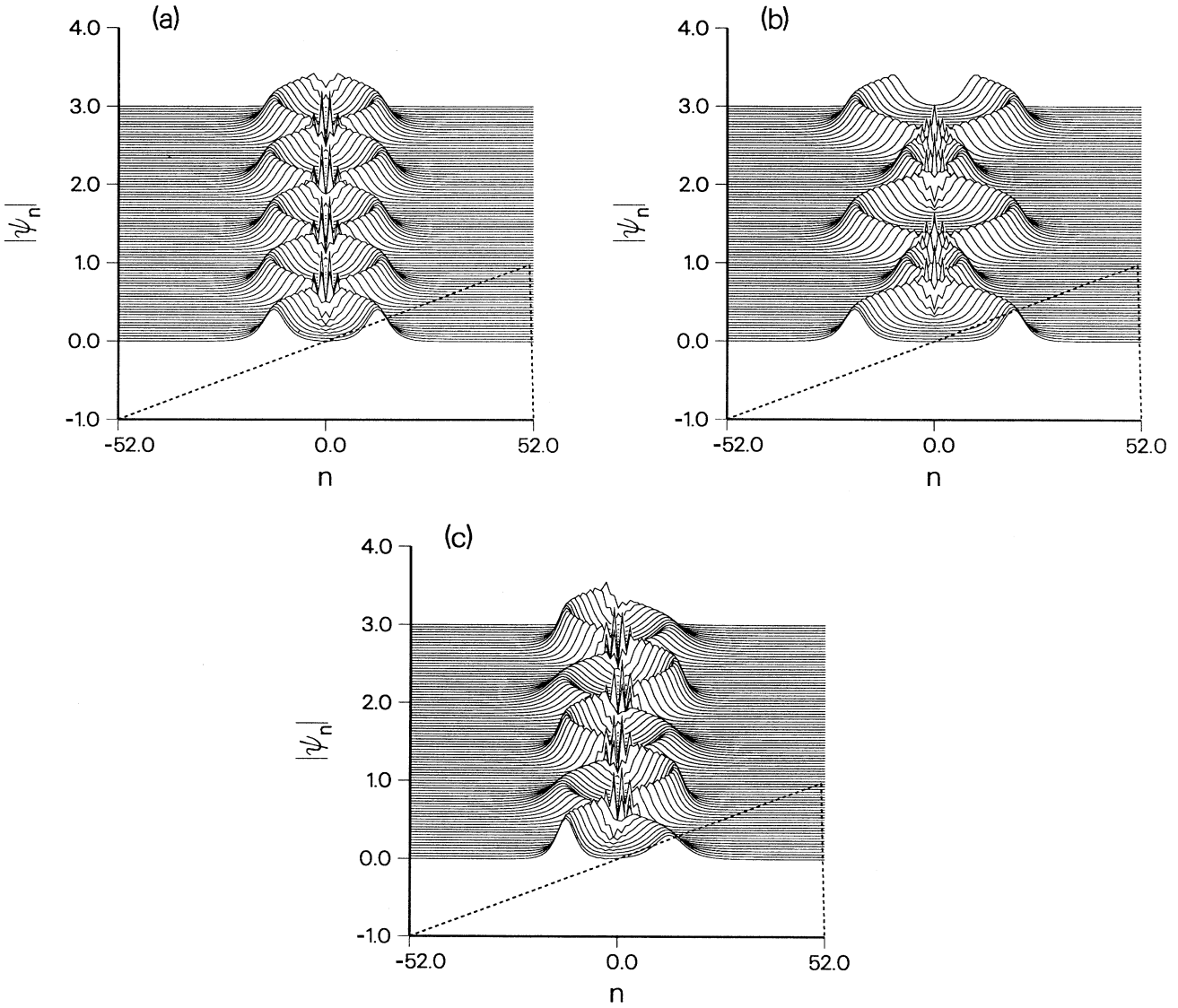

FIG. 5. Two-soliton collision on a tilted plane: Solution of Eq. (6), for $l_{\text{chain}}=104$; zero boundary conditions; $V_n=16n/l_{\text{chain}}$; initial soliton parameters: $\alpha_1=\pi$, $\alpha_2=0$, (a) and (b) $\beta_1=\beta_2=0.4$, and (c) $\beta_1=0.5$ and $\beta_2=0.3$; integration time $T=90$.

VI. TRAPPING ON AN IMPURITY

Now we turn to another interesting set of phenomena which can be investigated by a collective variable approach: the trapping of a soliton by an impurity potential $V_n = V\delta_{n,0}$. Stationary solutions are readily found by matching parts of stationary solitons ($\alpha=0$) for $V=0$ having the same frequency $\omega=-2\cosh\beta$:

$$\psi_n(t)=\sinh\beta\,\mathrm{sech}\{\beta[|n|-\mathrm{sgn}(V)\xi]\}e^{-i\omega t}\ , \tag{27}$$

where $\xi>0$ and $\cosh\beta\xi=2\sinh\beta/(\omega^2-4-V^2)^{1/2}$. For an attractive impurity ($V<0$), the solution ψ_n has a maximum at $n=0$; for a repulsive impurity ($V>0$), it has a minimum at $n=0$ between maxima at $\pm n_0\approx\xi$. For $V=0$ the original soliton with $\xi=0$ is restored. In all cases one finds

$$|\psi_{n=0}(t)|^2=\frac{\omega^2-4-V^2}{4}\ , \tag{28}$$

showing that solutions (27) exist only for sufficiently large β: $\sinh\beta\geq|V|/2$.

Two remarks should be made. First, looking for staggered solutions of Eq. (6) with the form $\psi_n(t)=(-1)^n\tilde{\psi}_n(t)$, one immediately verifies that $\tilde{\psi}_n(-t)$ is also a solution of Eq. (6), but with V_n replaced by $-V_n$. In contrast, Eq. (1) does not possess this exact symmetry. For staggered solutions, Eq. (27) has to be changed to

$$\psi_n(t)=(-1)^n\sinh\beta\,\mathrm{sech}\{\beta[|n|+\mathrm{sgn}(V)\xi]\}e^{i\omega t}\ . \tag{29}$$

Impurities acting repulsively on the unstaggered solution (27) act attractively on the staggered solution (29) and vice versa.

The second remark concerns the integrals E and N. If we denote $\psi_n^{\pm}(t)$ the solution (27) for $V=\pm|V|$, and $E_{\pm},N_{\pm}$ their corresponding integrals, we find

$$\begin{aligned} N_+ + N_- &= 2N_0 = 4\beta\ , \\ E_+ + E_- &= 2E_0 = -4\sinh\beta\ , \end{aligned} \tag{30}$$

where the potential energy terms in the last line have canceled. We observe that $N_-<N_0<N_+$. For integer ξ, energies and norms may be expressed in closed form.

What really happens dynamically in the vicinity of the impurity cannot be determined by investigating trapped oscillatory solutions alone [as given by Eq. (27) or (29)]: There may be scattering and emission of phononlike excitations as well as multisoliton processes. To simplify matters we choose a soliton at rest ($\alpha=0$ or π) on top of the impurity and assume that the main decay channel is through generation of two solitons. As the initial condition is symmetric with respect to spatial inversion, we expect the two solitons to have the same shape but opposite velocity. Initially, we have for the norm $N=2\beta$ and for the energy $E=\mp4\sinh\beta+2V\ln(\cosh\beta)$ for $\alpha=0$ or π. Well after the decay into two traveling solitons (and hopefully negligible radiation) with exponentially small overlap with the impurity, we find for the norm $N'=4\beta'$ and for the energy $E'=-8\sinh\beta'\cos\alpha'$. If we assume that the amount of radiation emitted during the decay is negligible ($N=N'$, $E=E'$) we find

$$\cos\alpha'=\pm\cosh(\beta/2)-\frac{V\ln(\cosh\beta)}{4\sinh(\beta/2)}\ , \tag{31}$$

where $\pm$ refers to $\alpha=0$ or π (staggered initial solution). If α' approaches one of the critical values 0 or π, the emission of the two solitons is slowed down: $u'\to0$. In the limit, the two-soliton decay is prohibited. If initially $\alpha=0$, then the two-soliton decay is possible for

$$\begin{aligned} 0<&\frac{4\sinh(\beta/2)[\cosh(\beta/2)-1]}{\ln(\cosh\beta)} \\ <V<&\frac{4\sinh(\beta/2)[\cosh(\beta/2)+1]}{\ln(\cosh\beta)}\ . \end{aligned} \tag{32}$$

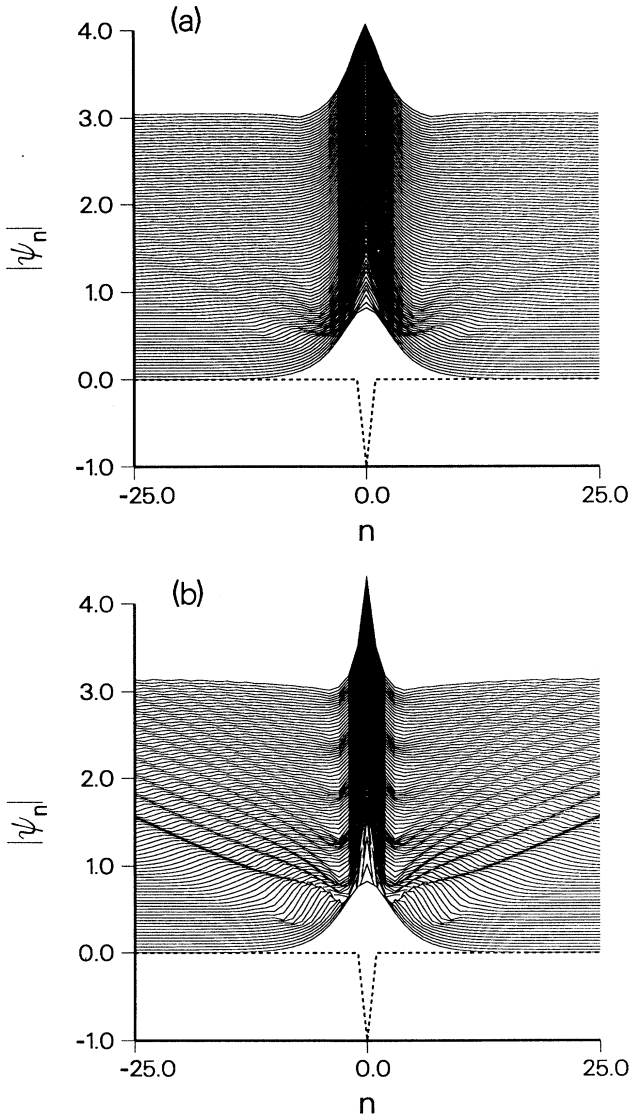

FIG. 6. Soliton trapping on an attractive impurity: Solution of Eq. (6), for $l_{\mathrm{chain}}=314$; periodic boundary conditions, $V_n=V\delta_{n,0}$; initial soliton parameters: $\beta=0.4$, $\alpha=0$; (a) $V=-0.3$ and (b) $V=-2.0$; integration time $T=30$; $|\psi|$ magnification 2×.

If initially $\alpha=\pi$, then the two-soliton decay is possible for

$$-\frac{4\sinh(\beta/2)[\cosh(\beta/2)+1]}{\ln(\cosh\beta)} < V < -\frac{4\sinh(\beta/2)[\cosh(\beta/2)-1]}{\ln(\cosh\beta)} < 0 . \quad (33)$$

In the continuum limit the bounds in Eq. (32) go to $\beta/2$ and $+\infty$, and in the "staggered" continuum limit the bounds in Eq. (33) go to $-\infty$ and $-\beta/2$.

Trapping on an arbitrarily large repulsive impurity as given by Eqs. (27) and (29) is a static nonlinear effect. It turns out that dynamically these trapped states are stable only up to a given threshold approximately given by Eqs. (32) and (33), beyond which they break up into two solitons and radiation.

For an unstaggered initial soliton ($\alpha=0$) the following picture emerges. If $V<0$, no two-soliton decay is possible. The soliton adjusts to the exact solution (27) with one maximum by emitting radiation. If $|V|\leq 2\sinh\beta$, the amount of radiation will be relatively small (the matching condition at the impurity can be fulfilled by a solution with unchanged β). In the opposite case the soliton has to adjust to a state with $\beta'>\beta$ and more radiation will be emitted. If $V>0$, but less than the first threshold in Eq. (32), it oscillates around the exact solution (27) with two maxima. If V lies well between the two thresholds in Eq.

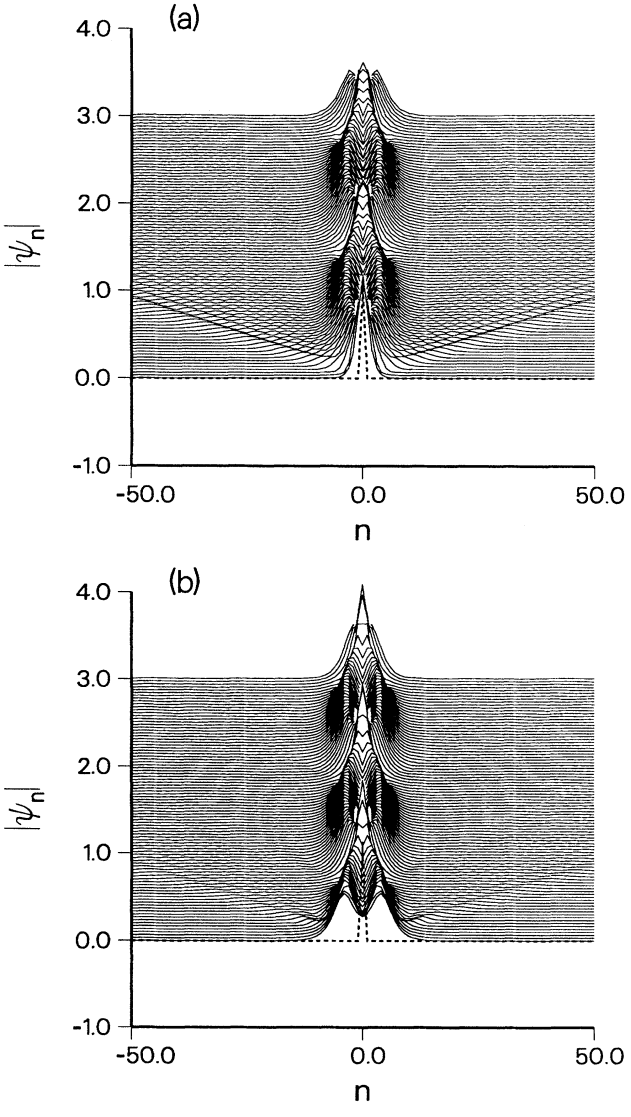

FIG. 7. Soliton trapping on a repulsive impurity: Solution of Eq. (6), for $l_{\text{chain}}=314$; periodic boundary conditions; $V_n=V\delta_{n,0}$, $V=0.67$; initial soliton parameters: (a) $\beta=1.0$, $\alpha=0$; (b) superposition of two solitons with $\beta=0.5$, $\alpha=0$, $x_0=\pm 4$; integration time $T=90$.

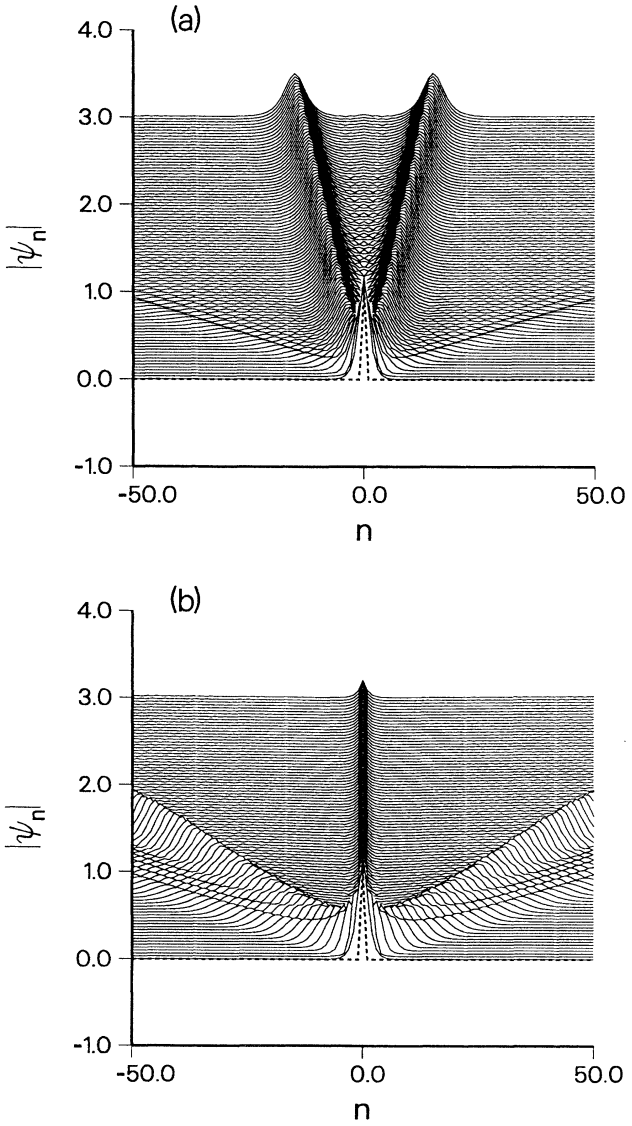

FIG. 8. Soliton on a strong, repulsive impurity: Solution of Eq. (6), for $l_{\text{chain}}=314$; periodic boundary conditions; $V_n=V\delta_{n,0}$; initial soliton parameters: $\beta=1.0$, $\alpha=0$; (a) $V=0.70$ and (b) $V=2.0$; integration time $T=90$.

(32), two-soliton decay is possible. The upper threshold is usually too large to be of practical importance because the radiation effects are no longer negligible if V becomes too large.

Figure 6 illustrates trapping and adjustment for $V<0$ (i.e., an *attractive* impurity). For $|V| \leq 2\sinh\beta$, adjustment with a negligible amount of radiation occurs [Fig. 6(a)], whereas Fig. 6(b) shows the opposite case. Figure 7 shows the case $0<V<V_c$, where $V_c \approx 0.7$ denotes the lower bound in Eq. (32), leading to a trapped oscillating two-soliton state. Initial conditions are a one-soliton state in Fig. 7(a) and the superposition of two one-soliton states with $\beta'=\beta/2$ and $x_0=\pm 4$ in Fig. 7(b) for comparison. Figure 8 illustrates the case $V>V_c$, leading to two unbound solitons [Fig. 8(a)] and, in addition to that, to a trapped staggered state for larger values of V [Fig. 8(b)]. (Staggered states can be trapped on impurities with arbitrarily large positive V.) Numerical evidence shows that the value for V_c as determined by Eqs. (32) and (33) is typically 10% too small, indicating the influence of radiative losses.

It is interesting to compare V_c here with the crossover suggested in disordered "polaron" problems (with electron-phonon, exciton-phonon,[16] magnon-phonon coupling) discussed by Anderson[17] and others.[18] These authors have considered the competition of disorder and nonlinearity localization within a stationary approximation [$\psi_n(t)=\exp(-i\omega t)\chi_n$], whereas here we have explored the full time dependence.

VII. SUMMARY

In this article we have shown that the nonlinear Schrödinger equation on a lattice with on-site potential has many interesting features lying beyond the reach of perturbation theory. Nevertheless, they can largely be understood in simple soliton collective-coordinate terms. Some of the features are novel and might give rise to interesting effects in physical systems with nonlinear interactions and when tight-binding approximations are applicable. Finite maximum soliton velocities and trapping of solitons on potential *maxima* were explained as novel discreteness effects and described in a collective variable approximation. The complete integrability for the discrete NLS equation with linear potential was demonstrated and proven. In this case the single soliton collective variable approximation turned out to be exact. We also described the trapping of a soliton on a *repulsive* δ-function impurity and its breakup for sufficiently large strength of the impurity. An approximation for the critical strength was calculated in the collective variable approximation. In the case of an attractive impurity, we observed a transition from a soliton state to a localized impurity mode upon increasing the strength of the impurity. We stress again that we considered here the full time-dependent behavior of the system and not only the stationary solutions.

The model we investigated is also a good starting point for clarifying the influence of periodic, quasiperiodic, and random[19] on-site potentials on the localization and transmission properties, as we will describe elsewhere. Preliminary results show that for small, random potentials there exists a critical velocity for traveling solitons below which they desintegrate rapidly and beyond which they travel long distances with negligible change of shape, leaving behind radiation that will finally be trapped in a (linear) Anderson sense.[20]

The model is also currently under investigation for a time-dependent, kicked potential. This leads to chaotic or regular motion of a single soliton (depending on the initial conditions), which, in a single soliton collective variable approximation, can be described by a nonintegrable symplectic map (similar to the standard map). Sensitive dependence on initial conditions and existence of soliton-like solutions together give rise to new and interesting effects[21] (see also Refs. 22 and 23).

Finally, the properties of this dynamics illustrate the fact that complete integrability of a system with infinitely many degrees of freedom is not necessary to support simple, stable, and localized solutions in space and time.

ACKNOWLEDGMENTS

We thank F. Abdullaev, Y. Kivshar, and P. Lomdahl for valuable help and advice, and acknowledge support by the U.S. Department of Energy and NATO Grant No. RG674-88.

[1] *Disorder and Nonlinearity,* edited by A. R. Bishop, D. K. Campbell, and S. Pnevmatikos (Springer-Verlag, Berlin, 1989).

[2] A. Hasegawa, *Optical Solitons in Fibers* (Springer-Verlag, Berlin, 1989).

[3] N. Mott, *Conduction in Non-Crystalline Materials* (Oxford University Press, Oxford, 1987).

[4] *Electron-Electron Interaction in Disordered Systems,* edited by A. L. Efros and M. Pollak (North-Holland, Amsterdam, 1985).

[5] *Solitons,* edited by S. E. Trullinger, V. E. Zakharov, and V. L. Pokrovsky (North-Holland, Amsterdam, 1986).

[6] J. C. Eilbeck, P. S. Lomdahl, and A. C. Scott, Physica D **16**, 318 (1985).

[7] A. C. Scott, Philos. Trans. R. Soc. London A **315**, 423 (1985).

[8] B. M. Herbst and M. J. Ablowitz, Phys. Rev. Lett. **62**, 2065 (1989).

[9] Y. Wan and C. M. Soukoulis, Phys. Rev. A **41**, 800 (1990).

[10] *Dynamical Systems III,* edited by V. I. Arnold, (Springer-Verlag, Berlin, 1988).

[11] M. J. Ablowitz and J. F. Ladik, J. Math. Phys. **17**, 1011 (1976).

[12] L. D. Faddeev and L. A. Takhtajan, *Hamiltonian Methods in the Theory of Solitons* (Springer-Verlag, Berlin, 1987).

[13] Y. S. Kivshar and B. A. Malomed, Rev. Mod. Phys. **61**, 763 (1989).

[14] R. Balakrishnan, Phys. Rev. A **32**, 1144 (1985).

[15] H.-H. Chen and C.-S. Liu, Phys. Rev. Lett. **37**, 693 (1976).

[16]H. Feddersen, Phys. Lett. A **154**, 391 (1991).
[17]P. W. Anderson, Nature **235**, 163 (1972).
[18]M. H. Cohen, E. N. Economou, and C. M. Soukoulis, Phys. Rev. Lett. **51**, 1202 (1983).
[19]J. G. Caputo, A. C. Newell, and M. Shelley (unpublished).
[20]R. Scharf and A. R. Bishop (unpublished).
[21]R. Scharf (unpublished).
[22]I. S. Aranson, K. A. Gorshkov, and M. I. Rabinovich, Phys. Lett. A **139**, 65 (1989).
[23]F. Benvenuto, G. Casati, A. S. Pikovsky, and D. L. Shepelyansky (unpublished).